Gene Therapy (2008) 15, 155–160

www.nature.com/gt

ORIGINAL ARTICLE

Myostatin antisense RNA-mediated muscle growth in normal and cancer cachexia mice

C-M Liu[1,3], Z Yang[1,3], C-W Liu[1], R Wang[1], P Tien[1], R Dale[2] and L-Q Sun[2]
[1]Molecular Virology Research Center, Institute of Microbiology, Chinese Academy of Sciences, Beijing, China and [2]Oligos Etc Inc., Wilsonville, OR, USA

Myostatin is a negative regulator of myogenesis, and inactivation of myostatin leads to muscle growth. Here we have used modified RNA oligonucleotides targeting the myostatin mRNA and examined the therapeutic potential in normal and cancer cachexia mouse models. We found that the RNA oligonucleotides could suppress the myostatin expression in vivo, *leading to the increase in muscle growth both in normal and cachectic mice. We also established that the effect of myostatin inhibition caused by the RNA oligonucleotides may be through the MyoD pathway, as evidenced by a significant upregulation of MyoD expression. Taken together, these results demonstrate the feasibility using antisense strategy for the treatment of muscle wasting conditions.*
Gene Therapy (2008) **15,** 155–160; doi:10.1038/sj.gt.3303016; published online 22 November 2007

Keywords: *myostatin; antisense; muscle wasting; cancer cachexia*

Introduction

Conditions involving muscle wasting or related to abnormalities of body composition are widespread and include muscular dystrophy, spinal cord injury, neurodegenerative diseases, sarcopenia, cachexia, atrophy due to immobilization, bed rest or weightlessness, and diabetes mellitus.[1] These conditions involve a decrease in muscle mass with concomitant loss of strength and function and can lead to disability and, in extreme cases, death, often as a direct or indirect result of lack of skeletal muscle mass and strength. These conditions are often multifactorial in origin and can involve abnormal expression of multiple genes in multiple pathways.[2]

Myostatin is a major gene involved in regulating muscle growth that may be involved, directly or indirectly, in almost every muscle wasting condition.[3] As a secreted growth factor, myostatin acts as a negative regulator of skeletal muscle mass in mammals and other animals. Myostatin is almost exclusively expressed in the skeletal muscle lineage, where it negatively regulates myocyte differentiation/growth and determines muscle size. It is a member of the transforming growth factor-β family and is expressed in both developing and adult muscles. Mice lacking the myostatin gene have 25–30% increased muscle mass.[4] Individual muscles, such as the pectoralis and quadriceps, of myostatin mutant mice are two- to threefold heavier than those of wild type mice.[5]

This modulation occurs both in early development and in adults. Blockage of myostatin function in adult mice using a myostatin antibody or conditional knockout technology results in an increment of muscle mass.[6] Since myostatin blockage is effective for increment of muscle mass even in adults, myostatin blockers also appear promising for the treatment of dystrophy and other muscle wasting diseases. Here we use myostatin-targeted 2′-*O*-methyl antisense RNA and show that administration of the antisense molecules can increase the muscle weight both in normal adult mice and in a cancer cachexia mouse model. This effect is specific and is associated with the downregulation of the target gene myostatin and upregulation of the myostatin-modulated myogenic factor MyoD.

Results

Antisense RNA targeted to myostatin increased the mass of muscles in normal mice

We designed three antisense oligonucleotides targeted at the 5′ untranslated region, start site and termination site on the basis the mouse myostatin mRNA sequence (NM010834). The sequences of the molecules are ATG TAGCGTCCGAGAGAC (702), TGCATCATTTTAAAAA TCAGC (703) and ACCTAATGCAAAGCTCAT (704). A control oligonucleotide was also designed on the basis of an irrelevant sequence. The backbones for all the oligonucleotides are phosphodiester linkages. In order to increase the stability *in vivo*, all the oligonucleotides were chemically modified by 2′-*O*-methyl and with a butanol tag at the 3′-end of each molecule. To examine the effect of these oligos on muscle growth, the antisense

Correspondence: Professor P Tien, Molecular Virology Research Center, Institute of Microbiology, Chinese Academy of Sciences, Beijing 100080, China. E-mail: tienpo@sun.im.ac.cn or Dr L-Q Sun, Oligos Etc Inc., 9775 SW Commerce Circle C6, PO Box 727, Wilsonville, OR 97070, USA.
E-mail: lsun@oligosetc.com
[3]These authors contributed equally to this work.
Received 1 November 2006; revised 30 July 2007; accepted 1 August 2007; published online 22 November 2007

RNAs were injected into normal mice through intravenous (i.v.) routes at the dose of 5 mg kg^{-1}, twice weekly for 4 weeks. Two days after the last injection, the leg muscles were weighed and the ratio of the leg's muscle weight to body weight in each group was calculated. As shown in Figure 1, all the antisense RNAs could increase the muscle mass with 703, 704 and mixed oligonucleotides showing statistically significant effect ($P<0.05$; Figure 1a). When a ratio of muscle mass to body weight was measured, a similar trend was observed in that the RNA oligonucleotides 703, 704 and mixed RNA showed a significant increase in the ratio ($P<0.05$; Figure 1b). To confirm that the effects of the RNAs on the muscle weight were associated with the target genes, quantitative real time-PCR (QRT-PCR) was performed to measure the target gene expression in the muscle of all the groups. As shown in Figure 1c and d, the mRNA level of myostatin decreased significantly in the groups treated with 704 and mixed RNAs ($n=8$, $P<0.05$), while the MyoD mRNA increased markedly only in the mixed RNA group but not in the 704 group, compared to the saline control group ($n=8$, $P<0.05$). Although we could not explain why the 704 RNA oligonucleotide could downregulate myostatin expression and increase the muscle growth, but failed to show the effect on MyoD expression, the timing of collection of total RNA from the

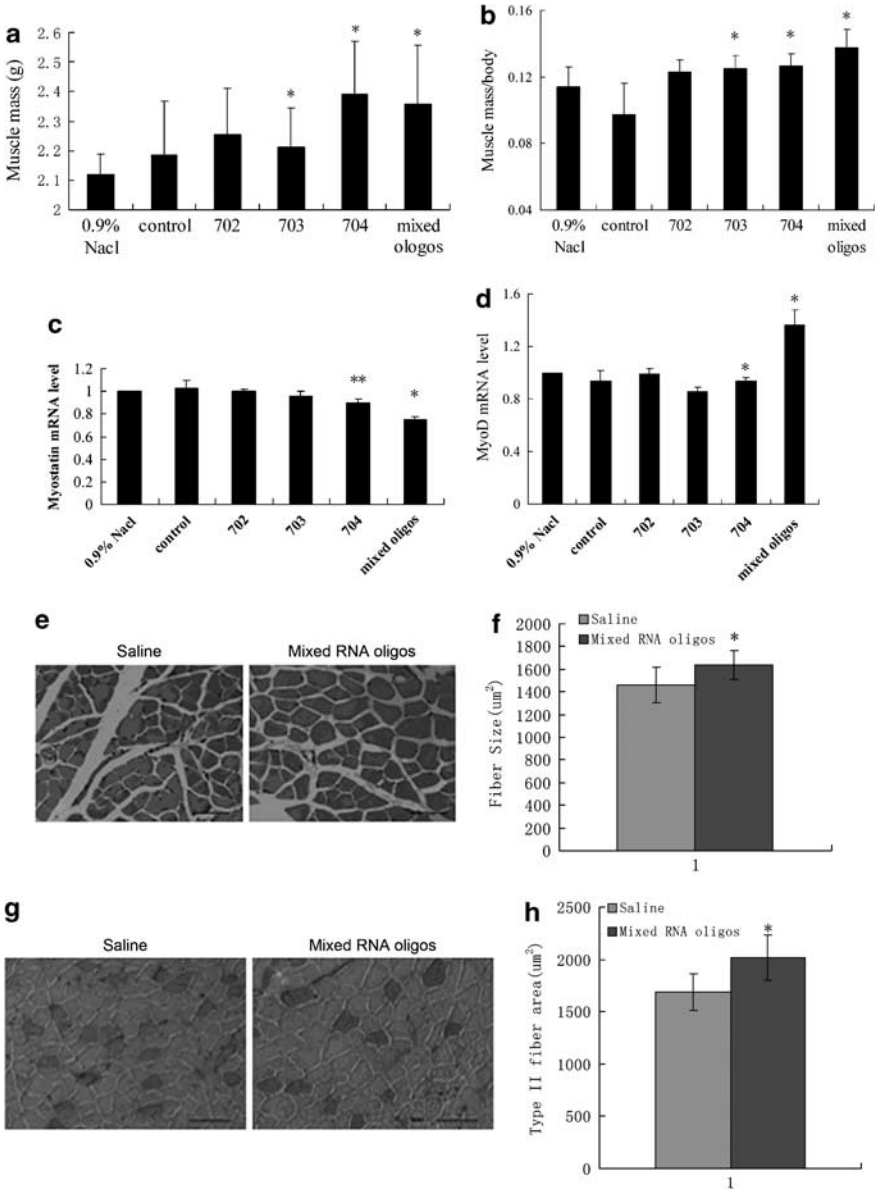

Figure 1 Effect of myostatin antisense RNA on muscle growth and target gene expression. (**a**) Muscle weight ($P<0.05$ vs 0.9% NaCl control group). (**b**) Ratio of muscle mass to body weight ($P<0.05$ vs 0.9% NaCl control group). (**c**) Quantitative RT-PCR analysis of myostatin expression at mRNA levels ($P<0.05$; **$P<0.01$ vs 0.9% NaCl control group). (**d**) Quantitative RT-PCR analysis of MyoD expression at mRNA levels ($P<0.05$). Data are mean ± s.d. ($n=8$). (**e**) Representative micrograph of muscle treated with saline (left) and mixed RNA oligos (right). Bar: 100 μm. (**f**) Gastrocnemius muscle fiber area determined by quantitative image analysis of six fields for each tissue section, *$P<0.05$. From each muscle sample, 500–700 fibers were analyzed. (**g**) Myofibrillar ATPase stained muscle cross-section. Fiber types were determined by staining intensity, type I>type II (from dark to light). Scale bar, 100 μm. (**h**) Comparison of type II fiber areas in gastrocnemius cross-sections from the mice treated with the mixed RNA oligonucleotides and control mice. $n=8$ per group. *$P<0.05$

tissue may be the reason for not being able to see the effect on MyoD.

Skeletal muscle is composed of postmitotic, multinucleated fibers. The increase in muscle mass observed with anti-myostatin treatment could result from the increased muscle fiber number or size. In order to determine the effect of antisense RNA on muscle fibers, we measured the fiber cross-sectional area in mixed RNA oligos treated and saline treated mice. Significant increases were noted in the single-fiber area of skeletal muscle from the mixed RNA oligos treated mice, indicating true hypertrophy at the single-myofiber level. Overall, in the mixed RNA oligos treated mice, the muscle fiber area was increased by 12.3% as compared to that in saline controls (Figure 1e and f). To further determine which type of fibers was responding to the downregulation of the myostatin expression, resulting in hypertrophy, a myofibrillar ATPase staining assay was performed. As shown in Figure 1g, the type II fiber areas (lighter staining) from the mice treated with the mixed RNA oligonucleotides were significantly increased, while the type I fiber areas (darker staining) showed no marked change. The mean value of the type II fiber area of the mice treated with the mixed RNA oligonucleotides was $2019 \pm 214\ \mu m^2$; the type II fiber area of the control mice was $1688 \pm 175\ \mu m^2$ (Figure 1f), which represented a 19.6% increase.

Together, these results demonstrated that the antisense RNA oligonucleotides could inhibit the myostatin expression, leading to the increase in muscle weight.

Myostatin antisense RNAs induced muscle growth in normal mice through different routes of administration

In order to compare the effects of different routes of delivery on the efficacy of the RNAs, the mixed RNAs were given to mice by three routes: i.v. , intraperitoneal (i.p.)+i.v. and orally at same dose. For the i.v. route, the antisense RNA was given via tail-vein injection twice weekly. In the group treated through i.p. and i.v., the mice were injected via i.p. and i.v. alternately twice weekly, while in the oral group the antisense RNA was given through gavages. When compared with each corresponding control, the RNAs administrated through all three routes increased the muscle weight and the muscle to body weight ratio, with the results in the i.v. and oral route groups showing statistical significance ($P<0.05$) (Figure 2).

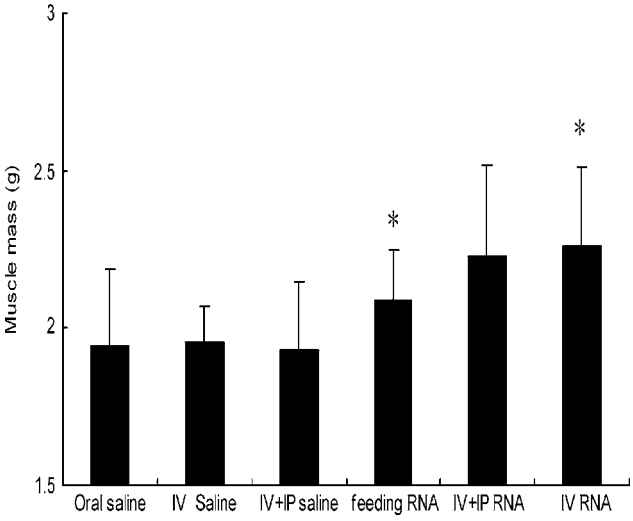

Figure 2 Comparison of different routes of administration. Mixed RNA oligos targeted to myostatin were given to mice through i.v., i.v./i.p. and oral (feeding) routes. The muscle weight was measured at the end of experiments and compared between each treatment group and its control, respectively. Data are presented as mean $\pm$ s.d. ($n=8$, $^*P<0.05$).

Myostatin expression increased in S-180 implanted mice

A cancer cachexia model can be established by inoculating ascitic tumors.[7] We chose the S-180 mouse ascitic tumor to create a cachexia disease model. We showed that after 14 days post inoculation, tumor-bearing mice significantly lost muscle weight (Figure 3a). Further molecular analyses demonstrated that in the muscle tissues of S-180 bearing mice, the myostatin mRNA expression level increased by 50% ($P<0.01$, Figure 3b) and MyoD expression decreased by 45.3% ($P<0.01$ Figure 3c) compared with normal mice. Western blotting results further confirmed that the protein expression pattern of myostatin and MyoD in S-180 implanted mice was in accordance with that of the mRNA level (Figure 3d). Thus, the S-180 implanted mice showed some characteristic features of cancer cachexia and could be used as a cachectic model.

RNA oligonucleotides targeted to myostatin decreased myostatin and increased the mass of muscles in the S-180 implanted mice

To explore the therapeutic potential of the myostatin RNA oligonucleotides, we tested the effect of the mixed RNAs on the muscle growth in the S-180 implanted mice. In the group injected with the mixed RNA targeted to myostatin, the muscle mass increased by 26% compared to the control group (Figure 4a, $P<0.05$), and the muscle to body weight ratio increased by 10.4% ($P<0.05$). When the muscle tissues were analyzed for the target gene expression, it was shown that the myostatin mRNA level decreased by 21.3% (Figure 4c, $P<0.01$) and the MyoD increased twofold compared to the saline control group (Figure 4d, $P<0.01$). This finding suggests that the antisense RNAs targeting myostatin mRNA can block the target gene expression in a sequence-specific manner and impact the pathological state in mice associated with an elevated myostatin level.

Discussion

Since its discovery, myostatin has quickly been established as a key regulator of skeletal muscle mass. The blockage of the myostatin expression holds great promise for the treatment of muscle wasting conditions. An anti-myostatin antibody (JA16) has been shown to increase muscle mass in healthy adult mice.[8] In the present study, we focused on the use of *in vivo* systems and showed that antisense RNA oligonucleotides could downregulate the target gene myostatin expression *in vivo*, leading to an increase of the muscle weight in normal mice. Our results further strengthen the notion that myostatin is an important therapeutic target for muscle wasting-related conditions.

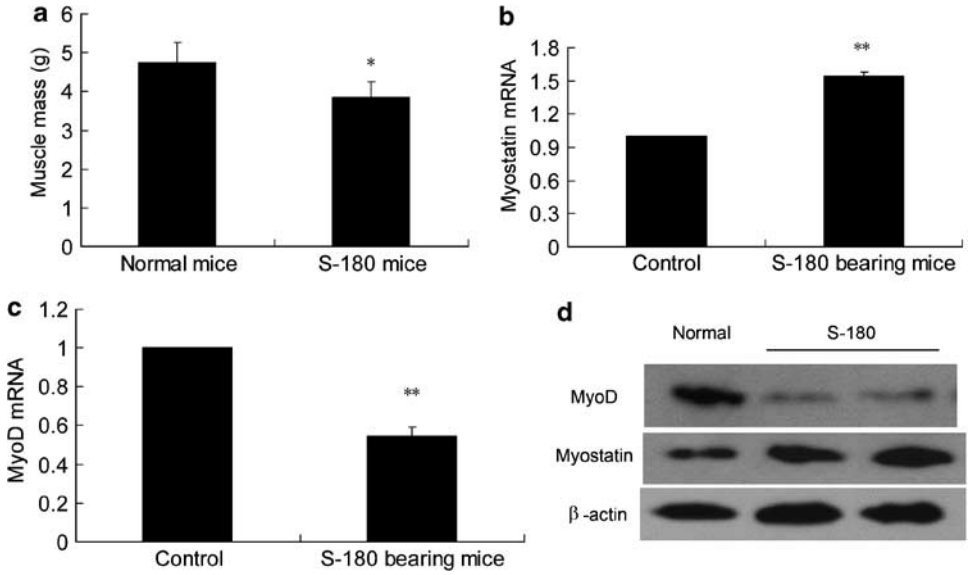

Figure 3 Characterization of S-180 bearing mice. (**a**) Muscle weight (*$P<0.05$); (**b**) quantitative RT-PCR for the expression of myostatin at mRNA level (**$P<0.01$); (**c**) Quantitative RT-PCR for the myoD expression at mRNA level (**$P<0.01$); (**d**) Comparison of myostatin and MyoD protein level in normal and S-180 implanted mice. Data are presented as mean ± s.d. ($n=8$).

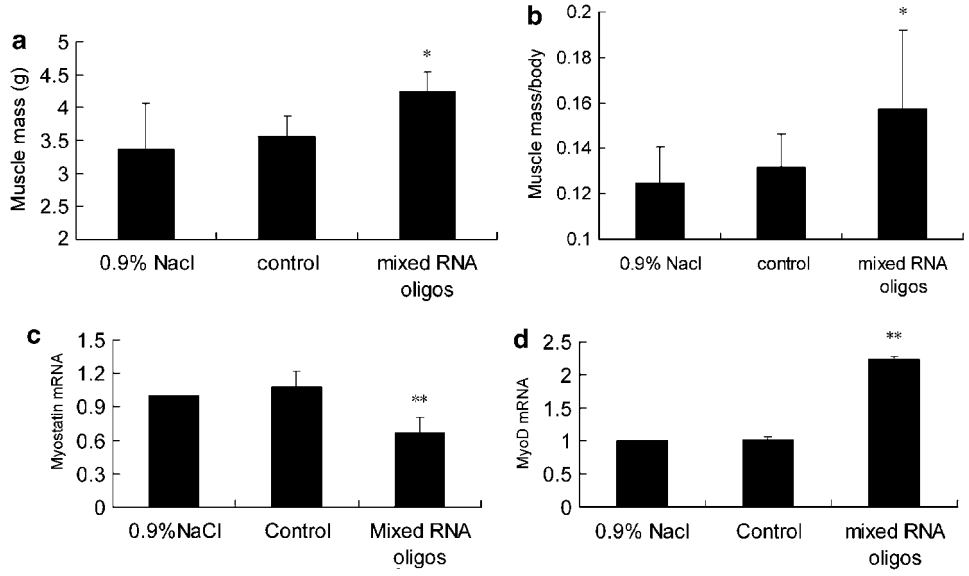

Figure 4 Antisense RNA effect on S-180 bearing mice. (**a**) Muscle weight at the end of the study (*$P<0.05$). (**b**) The ratio of muscle mass to body (*$P<0.05$). (**c** and **d**) Quantitative RT-PCR analysis of myostatin and MyoD expression at mRNA level in S-180 mice (**$P<0.01$). Data are presented as mean ± s.d. ($n=8$).

In addition to the use of antibody to inhibit the myostatin expression *in vivo*, there has been a report to employ vector-based small interfering RNA to regulate the myostatin expression. While the study demonstrated that local injection of a myostatin short hairpin RNA vetor into the muscle increased the muscle mass, this increase was only limited in the area where the injection occurred.[9] In our study, the myostatin antisense RNAs were administrated through more clinically relevant systemic routes (i.v., oral and i.p.) and produced significant effects on muscle growth.

Several reports showed that the level of myostatin increased in human aging associated with muscle wasting, and it may be a biomarker of age-associated muscle wasting and cachexia.[10–12] The cachexia associated with many chronic disease states, including cancer, AIDS (acquired immunodeficiency syndrome) and sepsis, contributes significantly to the morbidity and mortality associated with these diseases. Until now, no clinically effective drugs for cachexia have yet been developed.[13–14] In order to test our RNA oligonucleotides in a clinically relevant disease model, we employed an S-180 ascitic tumor from a mouse origin to establish a cancer cachexia model. In the tumor-bearing mice, there were some characteristic changes for muscle wasting conditions: upregulation of the myostatin expression as

determined by real-time PCR and western blots, and decrease in muscle weight. In this model, further testing of the RNA oligonucleotides, which showed some efficacy in normal mice, demonstrated that inhibition of myostatin by the antisense RNA could impact muscle growth in a cachectic condition.

Although myostatin has been considered to be one of the potential molecular targets for muscle wasting conditions, the regulators and pathways involved in the pathological process are largely unknown. It has been suggested that myostatin inhibits MyoD expression via Smad3 in C2C12 cells.[15] We speculate that the down-regulation of myostatin may lead to removal of the repression on MyoD expression, resulting in increase of cellular myogenic activities regulated by MyoD. In fact, each of the muscle regulatory factors, such as MyoD, Myf5, myogenin and MRF4, has the ability to convert non-muscle cell types into differentiation-competent myogenic cells after forced expression.[16,17] More recently, there have been reports revealing some direct action of myostatin on the myogenic factors.[18,19] In the current study, we did show that the inhibition of myostatin expression by antisense RNAs elevated the level of MyoD expression at the mRNA level *in vivo*. Thus, our results elucidate a possible mechanism for targeting the myostatin gene for potential treatment of the muscle wasting diseases and provide further evidence that myostatin regulates the muscle growth through the MyoD pathways.

Materials and methods

RNA oligos

The modified RNA oligonucleotides targeted to myostatin were synthesized and high-pressure liquid chromatography purified at Oligos Etc Inc., Oregon.

Animals

BALB/c female mice (6–8 weeks old) weighing 15–18 g were obtained from Institute of Genetics and Developmental Biology, Chinese Academy of Sciences, Beijing. The animals were housed for 1 week before starting the experiments. The animal experiments were undertaken within the guidelines of regulations for the use of experimental animals of Chinese Academy of Science.

RNA oligonucleotide treatment

In all the experiments, unless otherwise stated, the mice were administered with RNA oligonucleotides through tail vein or i.p. injection at the dose of 100 μg per 0.1 ml per injection twice weekly. For the use of the mixed oligonucleotides, the mixture was made at 33 μg of each three RNA oligonucleotides giving rise to a final dose of 100 μg per injection. The mice were weighed every day during the treatment period. At the end of the study, the leg muscles, including the quadriceps (rectus femoris), the gastrocnemius, the triceps and the EDL, were dissected and weighed. For oral administration, 100 μg RNA (100 μl) were given by gavages twice weekly.

Establishment of S-180 tumor bearing mice

S-180 cells (1×10^7) in 0.2 ml of phosphate-buffered saline were inoculated i.p. into BALB/C mice. The mice were fed with water and food normally for 2 weeks. The leg muscles, including the quadriceps (rectus femoris), the gastrocnemius, the triceps and the EDL, were dissected, weighed and freshly used for protein and mRNA extraction.

Quantitative RT-PCR analysis of mRNA

Total RNA was isolated from muscle tissues using RNA preparation kits from TRIZOL reagent (Invitrogen, CA, USA). cDNA was generated using ImpromIIreverse transcriptase (Promega, WI, USA) and oligo(d)T primers, according to the manufacturer's instructions. Typically, 1 μg of total RNA per reaction was used. Quantitative PCR was performed on an Applied Biosystems Prism 7000 instrument using Applied Biosystems SYBR® green master mix reagent (CA, USA). The primers (5′–3′) used in the PCR include:

Myostatin forward CAGACCCGTCAAGACTCCTACA
Myostatin reverse CAGTGCCTGGGCTCATGTCAAG
MyoD forward GCAAGACCACCAACGCTGAT
MyoD reverse GGTTCGGGTTGCTGGACGTG
β-Actin forward GAACCCTAAGGCCAACCGTGAA
β-Actin reverse CTCAGTAACAGTCCGCCTAGAA

Two negative controls consisting of mock reverse-transcribed cDNA (-RT) were included with each set of PCRs to exclude the possibility of genomic DNA contamination. The average C_T values for MyoD and growth differentiation factor (GDF-8) were calculated and normalized to C_T values for β-actin. The average C_t value from each of the three experiments was calculated, and the results were graphed with the corresponding standard deviation indicated with error bars in the figures. The formula and its derivations were obtained from the ABI Prism 7000 Sequence Detection System user guide.

Western blotting

Protein was extracted from the muscle tissue of different groups with lysis buffer containing 100 mM Tris HCl, 0.05% CA-630 100 μg ml^{-1} phenylmethylsulfonyl fluoride,100 μg ml^{-1} dithiothreitol, 1 μg ml^{-1} Aprotinin and 1 μg ml^{-1} Lenpeptin. Protein concentration of each specimen was determined by the Bradford method (Bio-Rad Laboratories, CA, USA) to ensure equal loading. Protein extracts were denatured at 95°C for 5 min, electrophoretically separated on a 12.5% sodium dodecyl sulfate-polyacrylamide gel electrophoresis and then transferred to a polyvinylidine difluoride membrane. The membrane was blocked with 5% non-fat dry milk in Tris-buffered saline with 0.1% Tween buffer (50 mM Tris HCl, 100 mM NaCl and 0.1% Tween-20, pH 7.4) and incubated with monoclonal anti-MyoD diluted at 1/200 (BD Pharmingen, CA, USA), monoclonal anti-myostatin diluted at 1/100 (Santa Cruz Biotechnology, CA, USA) and anti-β-actin diluted at 1/250(Santa Cruz Biotechnology), and was further incubated for 90 min at 37°C. Bound antibodies were visualized by subsequent chemiluminescent reaction with a horseradish peroxidase-conjugated IgG (1:6000) in the ECL system (Amersham, NJ, USA). The image and data were analyzed by Bandscan 5.0 software.

Histological analysis

Gastrocnemius muscles were removed from the mice and either fixed in formalin and embedded in paraffin or frozen. Paraffin sections (2–4 μm) were stained with

hematoxylin and eosin. For fiber counting and measurement of the cross-sectional area, quantitative evaluation of stained sections for myofiber size was performed using the ImagePro 5.0.1 program software (Media Cybernetics, Silver Spring, MD, USA), coupled to an Nikon 80I microscope equipped with a Nikon DS-L1 digital camera, calibrated for spatial measurement and intensity. Fiber size was determined by measuring the area of each transversal myofiber per fixed area. Approximately 500–700 myofibers were measured for each gastrocnemius tissue sample.

ATPase staining

The muscle samples were obtained fresh, frozen in isopentane cooled in liquid nitrogen and stored at -80°C. They were sectioned on a cryostat and stained with adenosine triphosphatase (ATPase) using a modified method of Brooke and Kaiser (1970) for analysis of the mean fiber area and fiber type. Sections were incubated in an acid pre-incubation medium (95 mM CH3COONa, 99 mM KCl, pH 4.2), followed by an ATP incubation medium (2.8 mM ATP, 47.5 mM NaOH, 65 mM NaCl, 52.75 mM glycine, 37.8 mM $CaCl_2$, pH 9.4). Fiber types were distinguished by the intensity of staining (type I > type II). Quantitative evaluation of stained sections for myofiber size was performed using the ImagePro 5.0.1 program software (Media Cybernetics), coupled to an Nikon 80I microscope equipped with a Nikon DS-L1 digital camera, calibrated for spatial measurement and intensity. Fiber size was determined by measuring the area of each transversal myofiber. From each muscle sample, 500–700 fibers were analyzed.

Statistical analysis

Data were expressed as means $\pm$ s.d. and subjected to one-way ANOVA with factors of treatment, disease or wild type. Comparisons between two groups were performed by unpaired Student's t test. A value of $P < 0.05$ was considered significantly different.

References

1 Lecker SH, Solomon V, Mitch WE, Goldberg AL. Muscle protein breakdown and critical role of the ubiquitin-proteasome pathway in normal and disease states. *J Nutr* 1999; **129**: 227S–237S.
2 Jackamn RW, Kandarian SC. The molecular basis of skeletal muscle atrophy. *Am J Physiol Cell Physiol* 2004; **287**: C834–C843.
3 Gonzalez-Cadavid NF, Bhasin S. Role of myostatin in metabolism. *Curr Opin Clin Nutr Metab Care* 2004; **7**: 451–457.
4 McPherron AC, Lawler AM, Lee SJ. Regulation of skeletal muscle mass in mice by a new TGF-beta superfamily member. *Nature* 1997; **387**: 83–90.
5 Grobet L, Pirottin D, Farnir F, Poncelet D, Royo LJ, Brouwers B *et al*. Modulating skeletal muscle mass by postnatal, muscle-specific inactivation of the Myostatin gene. *Genesis* 2003; **35**: 227–238.
6 Bogdanovich S, Krag TO, Barton ER, Morris LD, Whittemore LA, Ahima RS *et al*. Functional improvement of dystrophic muscle by myostatin blockade. *Nature* 2002; **28**: 418–421.
7 Baracos VE, DeVivo C, Hoyle DH, Goldberg AL. Activation of the ATP-ubiquitin proteasome pathway in skeletal muscle of cachectic rats bearing a hepatoma. *Am J Physiol* 1995; **268**: E996–E1006.
8 Whittemore LA, Song K, Li X, Aghajanian J, Davies M, Girgenrath S *et al*. Inhibition of myostatin in adult mice increases skeletal muscle mass and strength. *Biochem Biophys Res Commun* 2003; **300**: 965–971.
9 Magee TR, Artaza JN, Ferrini MG, Vernet D, Zuniga L, Reisz-Porszasz S *et al*. Myostatin short interfering hairpin RNA gene transfer increases skeletal muscle mass. *J Gene Med* 2006; **8**: 1171–1181.
10 Yarasheski KE, Bhasin S, Sinha-Hikim I, Pak-Loduca J, Gonzalez-Cadavid NF. Serum myostatin-immunoreactive protein is increased in 60–92 year old women and men with muscle wasting. *J. Nutr Health Aging* 2002; **6**: 343–348.
11 Dasarathy S, Dodig M, Muc SM, Kalhan SC, McCullough AJ. Skeletal muscle atrophy is associated with an increased expression of myostatin and impaired satellite cell function in the portacaval anastamosis rat. *Am J Physiol Gastrointest Liver Physiol* 2004; **287**: G1124–G1130.
12 Gonzalez-Cadavid NF, Taylor WE, Yarasheski K, Sinha-Hikim I, Ma K, Ezzat S *et al*. Organization of the human Myostatin gene and expression in healthy men and HIV infected men with muscle wasting. *Proc Natl Acad Sci USA* 1998; **95**: 14938–14943.
13 Tsuchidak K. Activins, myostatin and related TGF-beta family members as novel therapeutic targets for endocrine, metabolic and immune disorders. *Curr Drug Targets Immune Endocr Metabol Disord* 2004; **4**: 157–166.
14 Lee SJ. Regulation of muscle mass by myostatin. *Annu Rev Cell Dev Biol* 2004; **20**: 61–86.
15 Joulia D, Bernardi H, Garandel V, Rabenoelina F, Vernus B, Cabello G. Mechanisms involved in the inhibition of myoblast proliferation and differentiation by myostatin. *Exp Cell Res* 2003; **286**: 263–275.
16 Edmondson DG, Olson EN. A gene with homology to the myc similarity region of MyoD1 is expressed during myogenesis and is sufficient to activate the muscle differentiation program. *Genes Dev* 1989; **3**: 628–640.
17 Weintraub H, Tapscott SJ, Davis RL, Thayer MJ, Adam MA, Lassar AB *et al*. Activation of muscle-specific genes in pigment, nerve, fat, liver, and fibroblast cell lines by forced expression of MyoD. *Proc Natl Acad Sci USA* 1989; **86**: 5434–5438.
18 Kollias HD, Perry RL, Miyake T, Aziz A, McDermott JC. Smad7 promotes and enhances skeletal muscle differentiation. *Mol Cell Biol* 2006; **26**: 6248–6260.
19 Amthor H, Otto A, Macharia R, McKinnell I, Patel K. Myostatin imposes reversible quiescence on embryonic muscle precursors. *Dev Dyn* 2006; **235**: 672–680.